# Effect of post-thermal annealing on the structural and optical properties of ZnO thin films prepared from a polymer precursor

Jijoy. P. Mathew[a)†], George Varghese[b)], and Jacob Mathew[a)]

[a)] *Thin Film Research Laboratory, Department of Physics, St. Berchmans College, Changanassery, Kerala* 686101, *India*
[b)] *Department of Physics, Calicut University, Thenjippalam, Kerala, India*

(Received 19 December 2011)

ZnO thin films were synthesised by a new method which uses polyvinyl alcohol (PVA) as the polymer precursor. The films are annealed at different temperatures and for different annealing times. The structural parameters, like grain size, lattice constants, optical band gap, and Urbach energy, depend on the annealing temperature and time. All the films possess tensile strain, which relaxes as the annealing temperature and time increase. The photoluminescence (PL) spectra contain only ultraviolet (UV) peaks at low temperature, but as the annealing temperature and time increase, we observe peaks at the blue and green regions with a variation in the intensities of these peaks with annealing temperature and time.

**Keywords:** stress, band gap, Urbach energy, photoluminescence

**PACS:** 81.15.Fg, 78.40.Fy, 81.40.Ef, 61.05.cp **DOI:** 10.1088/1674-1056/21/7/078104

## 1. Introduction

Zinc oxide is a II–VI compound semiconductor that crystallizes in a hexagonal wurzite structure. It has a wide band gap ($\sim 3.37$ eV), by which it has been recognized as a promising photonic material in the ultraviolet (UV) region. It can be used as transparent electrodes in display devices and in photovoltaics because it is a transparent conducting oxide with high optical transparency ($\sim 90\%$). ZnO is very abundant in nature, has high thermal and chemical stability, large excitonic binding energy ($\sim$ 60 meV), and is more resistant to radiation damage than other semiconductors such as ZnSe and GaN, making it a promising candidate for astronomical applications and in low threshold laser fabrication. ZnO doped with transition metal ions exhibits the room-temperature ferromagnetism property that is required for spintronics applications. Because of these unique properties and practical applications, much attention has been paid to the synthesis of ZnO thin films in the past few decades.[1−4]

So far, various deposition techniques, such as sputtering, molecular beam epitaxy chemical vapour deposition, and pulsed laser deposition, have been attempted to grow high-quality crystalline ZnO thin films. However, these techniques require sophisticated and expensive equipment for working at high vacuum or high temperature. Sol–gel dip coating deposition of these metal oxide films has been an increasingly active and versatile technique for thin film deposition, because the preparation from aqueous solution has many advantages, such as with low cost and low deposition temperature, compared with the other methods mentioned above and can therefore be easily scaled up in industry.

A few reports are available on the detailed studies of the effects of post deposition temperature and annealing time on optical properties such as the optical dispersion of ZnO thin films and the correlation with its structural properties.[5−7] In this article, we study the influence of post-thermal annealing on the structural and optical properties of ZnO thin films on glass substrates using the sol–gel dip coating method by analyzing the observed X-ray diffraction (XRD) patterns, UV absorption spectra, and photoluminescence (PL) spectra.

†Corresponding author. E-mail: mathew.jijoy@gmail.com

© 2012 Chinese Physical Society and IOP Publishing Ltd

## 2. Experimental

ZnO thin films were deposited by the sol–gel dip coating method. Zinc acetate dehydrate and poly vinyl alcohols (PVA) were used as the starting materials. The concentration of zinc acetate to PVA was kept at 0.5 M, and the glass substrates were precleaned in Extran then cleaned in acetone using an ultra-sonic cleaner and dried. The glass substrate was then dipped into the coating solution with a withdrawal speed of 10 cm/min and with a dipping delay of 30 s. Since the boiling point of PVA is 230 °C, heat treatment temperatures as high as 250 °C may be required for the solvent to vaporize completely out of the film. Therefore, the obtained film was dried at 250 °C for 10 min in a furnace to evaporate the organic residuals. The procedure was then repeated 10 times.

Thermal annealing is a widely used method to improve crystal quality and to study the structural defects in materials. In a semiconductor the process of annealing may change the structure and stoichiometric ratio of the material. Because the dislocations and other structural defects will move in the material, absorption or decomposition will occur in the surface. To study the effect of thermal annealing on the structural and optical properties of the grown films, we annealed the samples at 350 °C, 450 °C, and 550 °C. The samples were kept in a muffle furnace for 1 h in air and then the furnace was cooled to room temperature. In order to study the effect of annealing time, the film annealed for 450 °C is annealed at four different times 0.5, 1.0, 1.5, and 2.0 h.

The XRD patterns were obtained with XPERT-PRO PANalytical CuK$\alpha$ radiation ($\lambda$ = 1.5406 Å). The UV measurements were carried out at room temperature using a T90 UV-VIS spectrometer (PG Instruments) in the wavelength region 300–700 nm with a clean glass substrate in the reference beam. Room temperature PL spectral studies were carried out using a Schimadzu 530RFPC photometer.

## 3. Results and discussion

### 3.1. Structural studies

Figures 1 and 2 show the XRD patterns of as-grown ZnO thin films annealed at different temperatures and for different annealing times, respectively. The XRD patterns indicate a ZnO phase with a hexagonal wurzite structure. We can see from Fig. 1 that both the as-grown and annealed films have a polycrystalline structure with orientations at the (100), (002), (101), (102), (110), and (103) planes. All the films have the same crystal structure but the intensities of the XRD peaks and the full width at half maximum (FWHM) vary with annealing temperature and time. The increase in intensity of the diffraction peaks with annealing temperature and time may be due to the increase in the crystalline quality of the grown films. Furthermore, the XRD patterns reveal $a$ and $c$ axes-oriented growth in both sets of samples. This may be due to the use of solvents with high boiling points.[8] The sol–gel process is characterized by post-deposition crystallization and the preferential $c$ axis orientation is due to the initial nucleation process and the subsequent growth orientation at the film/substrate interface.[9] Moreover, it should be noted that the (002) direction of the hexagonal ZnO structure is the most thermodynamically favourable growth plane because it offers the lowest surface energy. In a recent review, Znaidi[10] accounts for the preferred $a$ axis orientation by giving the suggestion that, due to the thermal treatment, the matching between the amorphous silica and non polar (100) face became more subtle than that between any other faces and hence results in the development of $a$ axis orientation.

The average grain size ($D$) is calculated by using Scherer's formula[11]

$$D = 0.9\lambda/\beta\cos\theta, \tag{1}$$

where $\lambda$ is the wavelength of the X-Ray used and $\theta$ is the diffraction angle.

The grain size of the ZnO thin film increases with the increase in annealing temperature and time. This can be regarded as the merging process of ZnO nanoparticles induced from thermal annealing. In the case of ZnO nanoparticles, at high temperature, the zinc or oxygen defects at the grain boundaries favour the merging process by stimulating the coalescence of more grains during annealing.[7] Fang *et al.*[12] suggests that at high temperature, more energy should be available for the atoms to acquire so that they may diffuse and occupy the correct site in the crystal lattice, and grains with lower surface energy will grow larger at high temperature.

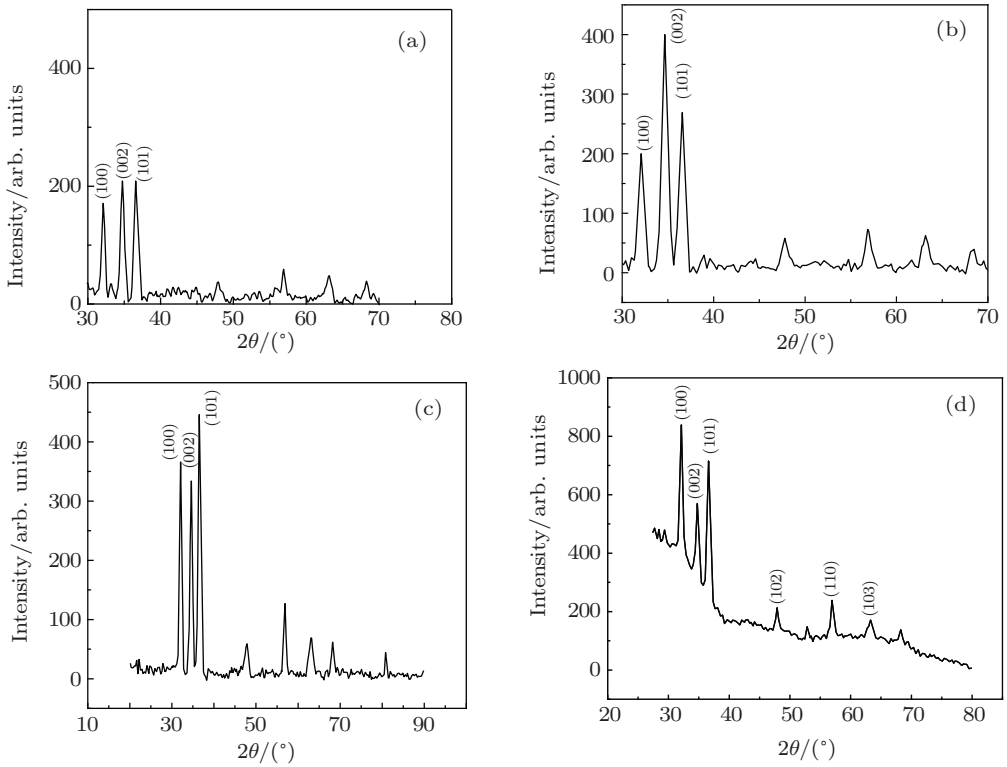



**Fig. 1.** XRD patterns of ZnO thin films annealed at different temperatures: (a) as-grown ZnO, (b) 350 °C annealed ZnO, (c) 450 °C annealed ZnO, (d) 550 °C annealed ZnO.

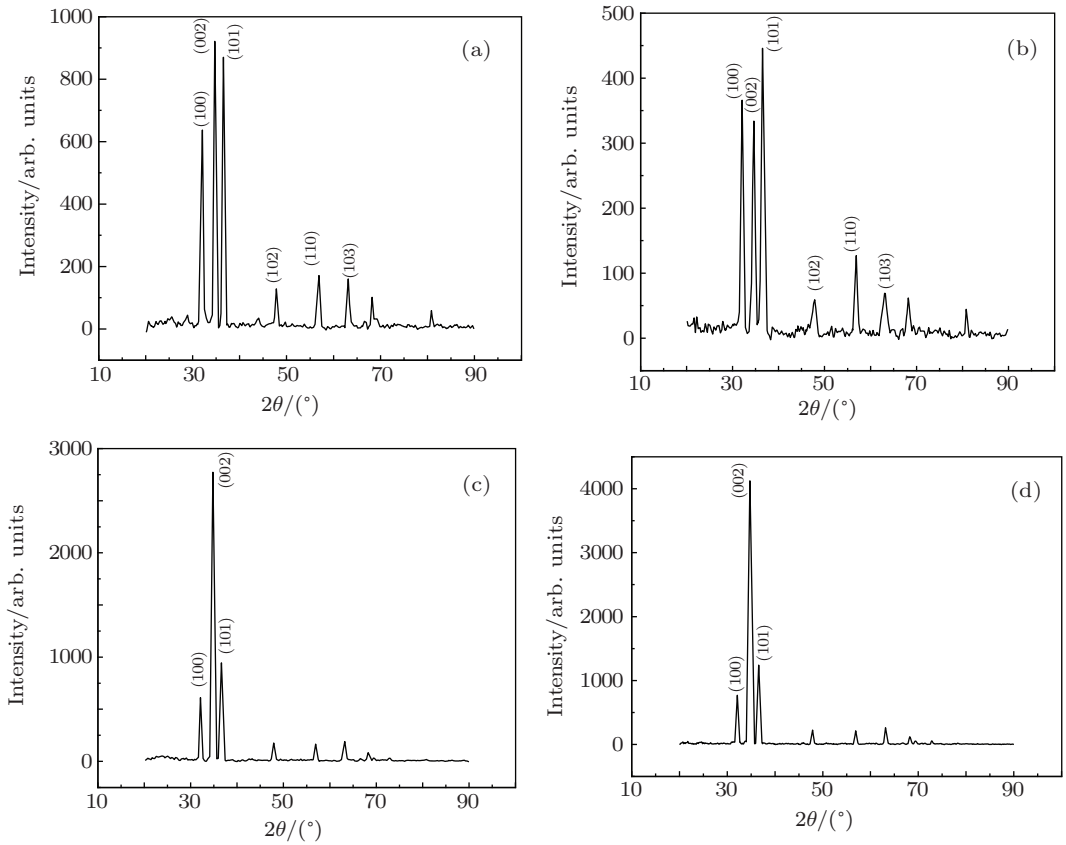



**Fig. 2.** XRD patterns of 450 °C annealed ZnO thin films for different annealing times: (a) 0.5 h, (b) 1.0 h, (c) 1.5 h, (d) 2.0 h.

As ZnO crystallizes in the wurzite structure in which the oxygen atoms are arranged in a hexagonal close packed type with zinc atoms occupying half the tetrahedral sites, Zn and O atoms are tetrahedrally coordinated to each other and therefore have an equivalent position. The zinc structure is open with all the octahedral and half the tetrahedral sites empty. According to Braggs law,

$$n\lambda = 2d\sin\theta. \tag{2}$$

For the hexagonal system, the lattice parameters $c$ of the samples were calculated using the formula[13]

$$1/d^2 = 4/3((h^2 + hk + k^2)/a^2)) + l^2/c^2, \tag{3}$$

where $h$, $k$, $l$ are Miller indices and $a$, $b$, and $c$ are the lattice parameters along the $x$, $y$, and $z$ directions. With the first order approximation $n = 1$, the lattice constant $a$ for the (100) plane is calculated by [14]

$$a = \lambda/\sqrt{3}\sin\theta. \tag{4}$$

For the (002) plane, the lattice constant $c$ was calculated by

$$c = \lambda/\sin\theta. \tag{5}$$

The lattice constants $a$ and $c$ of bulk ZnO were determined as $a = 3.24982$ Å and $c = 5.20661$ Å.

For our films we obtained lower values of $a$ and $c$ than the JCPDS values, and the values decrease as the annealing temperature and the annealing time increase. Similar results are also reported by other research groups.[14,15] This may be due to the lattice contraction resulting from the presence of dangling bonds on the surface of the ZnO films. The ions on the surface of the ZnO films are incompletely coordinated and possess unpaired electrons. These dangling bonds ($Zn^{2+}$ and $O^{2-}$ ions) form an electric dipole, resulting in a parallel array of dipoles originating in the boundary layer of each nanoparticle, which lies in this surface and experiences a repulsive force. ZnO has the property of absorbing $O^{2-}$ and $O^{-}$ ions in the surface, which increases the electrostatic attractive interaction between $Zn^{2+}$ and $O^{2-}$ ions, resulting in lattice contraction.

In the thermal annealed ZnO thin films, a shift of (002) peak position is observed with the increase in temperature. This indicates that the films are in a uniform state of stress with the tensile component parallel to the $c$ axis. Residual stresses are known to exist in thin films regardless of the type of deposition method. The electrical, optical and magnetic properties of ZnO thin films are known to be affected by these residual stresses present in the film. Therefore, we performed the strain and stress calculations using the values of the lattice parameters (strain $\varepsilon$ and stress $\sigma$) obtained from the XRD data[15]

$$\varepsilon = C_{\text{film}} - C_{\text{bulk}}/C_{\text{bulk}}, \tag{6}$$

$$\sigma = 2C_{13} - C_{33}(C_{11} + C_{12})/C_{13}, \tag{7}$$

where $C_{11} = 209.7$ GPa, $C_{12} = 121.1$ GPa, $C_{13} = 105.1$ GPa, and $C_{33} = 210.9$ GPa are the elastic stiffness constants of the bulk ZnO.[16]

We observe a tensile component of the intrinsic stress for all the prepared films. The angular peak positions are greater than the powder values associated with the tensile stress produced within the film.[17] The existence of tensile stress and strain in the prepared ZnO thin film is mainly due to lattice mismatch and thermal mismatch between the substrate and the thin film material. The thermal mismatch is due to the difference in thermal expansion coefficient ($\alpha$) between the ZnO ($\alpha_{\text{ZnO}} = 4 \times 10^{-6}$ K$^{-1}$) and glass substrate ($\alpha_{\text{Glass}} = 9 \times 10^{-6}$ K$^{-1}$).[16] Because of the large difference in the thermal expansion coefficient of the ZnO and that of the glass substrate, the substrate exerts a resultant tensile stress on the ZnO film as the substrate cools down from high temperature to low temperature. This tensile stress may be caused by the grain boundary relaxation. The residual tensile stresses are believed to result from grain growth when structural relaxation lags the deposition rate. The structural relaxation occurs to minimize the free energy of the system, resulting in a reduction of the specific volume of the film as long as the film is unconstrained. However, if the film is geometrically constrained by the substrate, volumetric relaxation is inhibited and a residual stress is produced in the film and substrate.[18,19]

To determine the band gap of the films, we use the equation in which the absorption coefficient $\alpha$ is related to the incident photon energy and band gap as

$$\alpha(h\nu) = A(h\nu - E_{\text{g}})^m,$$

where $A$ is a constant, $E_{\text{g}}$ is the optical band gap, and $m$ assumes the values of 1/2, 2, 3/2, and 3 for allowed direct, allowed indirect, forbidden direct, and forbidden indirect transitions.[20] The direct band gap

of the ZnO thin films is estimated from the extrapolation of the graph of $h\nu$ versus $\alpha^2$. Figures 3(a) and 3(b) show the curves of $h\nu$ versus $(\alpha h\nu)^2$ for ZnO thin films annealed at different annealing temperatures and for different annealing times, respectively. The optical band gap is found to be temperature dependent and the band gap decreases with the increases in annealing temperature and annealing time. The values of the band gap vary from 3.36 eV to 3.284 eV as the annealing temperature increases from 350 °C to 550 °C, and the band gap decreases from 3.39 eV to 3.10 eV as the annealing time increases from 0.5 h to 2 h.

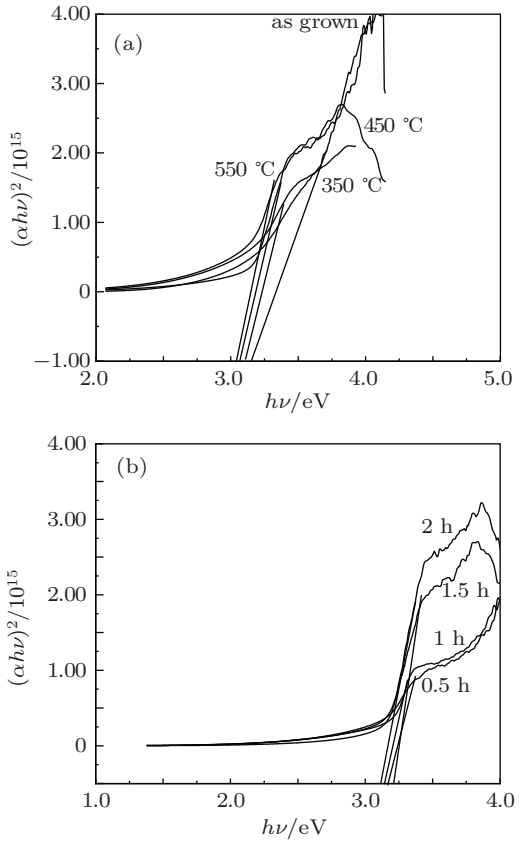



**Fig. 3.** The curves of $h\nu$ versus $(\alpha h\nu)^2$ for ZnO thin films annealed (a) at different temperatures and (b) for different annealing times.

Some researchers have reported that the band gap of ZnO thin films increases with the increase in temperature due to the effect of tensile strain. However, in our case, we observe a decrease in band gap with the increase in annealing temperature and annealing time. The decrease in the band gap may be due to the improved crystalline structure of the ZnO thin films with the increase in annealing temperature. Due to the disorder arrangements of the thin films grown at low temperature, the lowest states in the conduction bands are localized, called traps.[21] These traps will make the absorption edge shift to a higher energy by $\Delta E$, where $\Delta E$ is known as the mobility edge where the states become neither localized nor extended. Reference [21] gives a figure to illustrate the electronic structure of the amorphous semiconductors. At low temperatures, the amorphous nature of the ZnO phase increases. As a result, the extended localization in the conduction and valance band increases. Thus, the absorption edge will be mainly attributed to the amorphous ZnO and the films at lower temperature will have larger band gaps than the films grown at higher temperatures, and the band gap decreases as the temperature increases due to the decrease in the amorphous nature of ZnO.[22] From the XRD results, it is clear that the lattice constants decrease with annealing temperature and are smaller than the amorphous structure of ZnO due to the long-range translational periodicity, and as a result the band gap decreases with the increase in temperature.[23]

The optical absorption coefficient $\alpha$ just below the band edge in insulators and semiconductors is found to vary exponentially with the incident photon energy. At a given temperature, $\alpha$ satisfies the relation[11]

$$\alpha = \alpha_0 \exp[(h\nu - E_0)/E_{\rm U}], \tag{8}$$

where $\alpha_0$ and $E_0$ are constants, $h\nu$ is the incident photon energy, and $E_{\rm U}$ is the Urbach energy, which is interpreted as the width of the band tail. The Urbach energy can be determined from the reciprocal gradient of the slope of the curve of $\ln\alpha$ versus $h\nu$. Figures 4(a) and 4(b) show the variation in $\ln\alpha$ with $h\nu$ for the ZnO thin films annealed at different temperatures and for different annealing times, respectively. The Urbach energy decreases with the increases in annealing temperature and time. The Urbach energy can be treated as an indicator of the presence of different types of impurities and disorders present on the prepared samples. These defects are originated during the film growth process, causing lattice disorders and generating stress in the film. Because for higher temperature and longer annealing time the atoms will have a higher energy to adjust their position in the lattice, the crystallinity and stress relaxes are improved. The XRD calculation supports these observations.

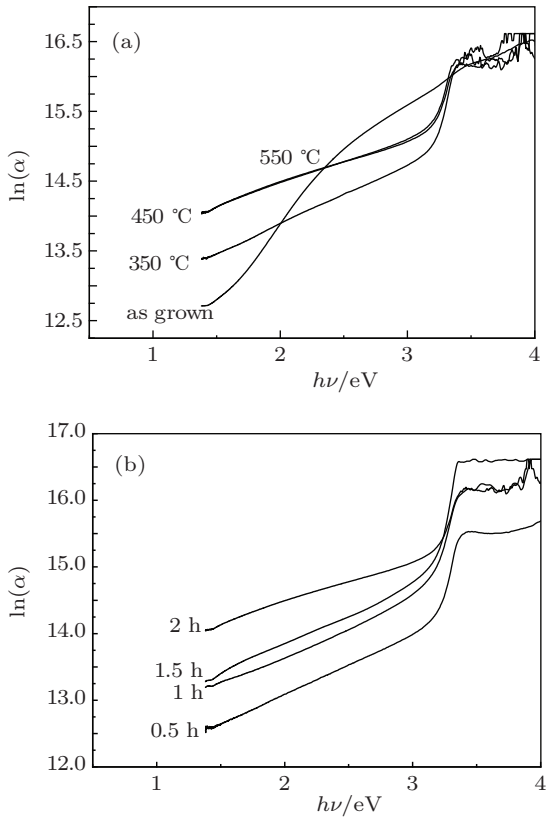



**Fig. 4.** The curves of $\ln\alpha$ versus $h\nu$ for ZnO thin films annealed (a) at different temperatures and (b) for different annealing times.

Figures 5(a) and 5(b) show the room temperature PL spectra of the ZnO films annealed at different temperatures and for different annealing times in the wavelength range of 300–700 nm. The PL spectra of as-grown and 350 °C annealed samples show peaks corresponding to the UV region. However, the PL spectra of the films annealed at 450 °C and 550 °C consist mainly of peaks at the UV, blue emission regions and small peaks or shoulders at blue–green region. For the samples annealed for different annealing times, the PL spectra are similar to those obtained for 450 °C annealing, but the intensities of the peaks change with time. As the annealing temperature increases, the peak positions are basically unchanged, but the intensity increases with the annealing temperature, which may be attributed to the increases in grain size and crystallinity. The UV and green emissions of the ZnO nanostructures and films have been extensively studied and the mechanisms for both are clearly known. The UV emission is attributed to the near band edge emission of the wide band gap of ZnO due to free excitonic transition.[24,25] The blue emission originates from the shallow donor level of oxygen vacancies to the valance band and the electron transition from the shallow donor level of the zinc interstitial to the valance band. The near green emission corresponds to the singly ionized oxygen vacancy in ZnO, which is supposed to be originated from the radial recombination of the photo-generated hole, with the electron belonging to the singly ionized oxygen vacancy.[26] According to the study of van Dijken *et al.*,[27] green emission may be due to the transition from the conduction band to the deeply trapped hole. However, according to the study of Lin *et al.*,[28] antisite oxygen can also induce green emission. The low density of the green emission may be due to the low density of oxygen vacancies, whereas the strong room temperature UV emission intensity should be attributed to the purity and crystallinity of the synthesized ZnO thin films. The structural and optical parameters of ZnO thin films annealed at different temperatures and for different annealing times is summarized in Tables 1 and 2, respectively.

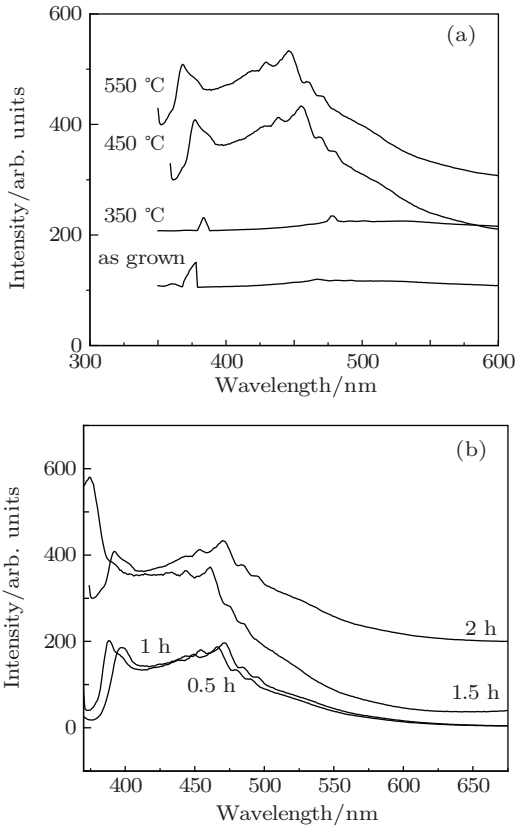



**Fig. 5.** PL spectra of ZnO thin films annealed (a) at different temperatures and (b) for different annealing times.

**Table 1.** The structural and optical properties of ZnO thin films annealed at different temperatures.

| Temperature/°C | $2\theta$ | $\beta$ | Particle size/nm | $a$/Å | $c$/Å | $c/a$ | Strain ($\varepsilon$) | Stress ($\sigma$)/$10^9$ Pa | Band gap/eV |
|---|---|---|---|---|---|---|---|---|---|
| as grown | 31.91 | 0.574 | 21.30 | 3.2358 | 5.1923 | 1.604 | .002439 | 0.568 | 3.36 |
| | 34.52 | 0.726 | | | | | | | |
| | 36.58 | 0.679 | | | | | | | |
| 350 | 31.97 | 0.482 | 23.99 | 3.2298 | 5.1893 | 1.606 | .00299 | 0.698 | 3.34 |
| | 34.54 | 0.724 | | | | | | | |
| | 36.57 | 0.576 | | | | | | | |
| 450 | 32.11 | 0.449 | 28.76 | 3.2167 | 5.1792 | 1.610 | .004953 | 1.154 | 3.30 |
| | 34.61 | 0.617 | | | | | | | |
| | 36.58 | 0.421 | | | | | | | |
| 550 | 32.139 | 0.195 | 37.20 | 3.2133 | 5.1575 | 1.605 | .009125 | 2.126 | 3.28 |
| | 34.76 | 0.368 | | | | | | | |
| | 36.59 | 0.381 | | | | | | | |

**Table 2.** The structural and optical properties of ZnO thin films annealed for different times.

| Time/h | $2\theta$ | $\beta$ | Particle size/nm | $a$/Å | $c$/Å | $c/a$ | Strain ($\varepsilon$) | Stress ($\sigma$)/$10^9$ Pa | Band gap/eV |
|---|---|---|---|---|---|---|---|---|---|
| 0.5 | 31.97 | 0.317 | 42.35 | 3.2298 | 5.1923 | 1.607 | .002439 | 0.568 | 3.39 |
| | 34.52 | 0.318 | | | | | | | |
| | 36.58 | 0.349 | | | | | | | |
| 1 | 32.11 | 0.449 | 28.76 | 3.2167 | 5.1792 | 1.610 | .004953 | 1.154 | 3.30 |
| | 34.61 | 0.617 | | | | | | | |
| | 36.58 | 0.421 | | | | | | | |
| 1.5 | 31.85 | 0.306 | 43.81 | 3.24174 | 5.1734 | 1.595 | .006067 | 1.413 | 3.26 |
| | 34.65 | 0.314 | | | | | | | |
| | 36.58 | 0.334 | | | | | | | |
| 2 | 32.07 | 0.306 | 42.30 | 3.22 | 5.14 | 1.62 | .012487 | 2.909 | 3.10 |
| | 34.65 | 0.313 | | | | | | | |
| | 36.58 | 0.350 | | | | | | | |

# 4. Conclusion

In summary, we prepared ZnO thin films from a polymer precursor and studied the effects of annealing time and temperature on the structural and optical properties of the film. It is observed that after annealing treatment, the ZnO films show a stronger intensity and narrower FWHM of the XRD peaks, thus improving the crystal quality of the films. All the films possess a tensile stress that increases with the annealing treatment. The optical properties of the films also depend on the annealing process. We have demonstrated that annealing treatment is an effective and efficient method to improve the crystallinity and optical properties of ZnO films.

# Acknowledgements

Jijoy. P. Mathew would like to express sincere thanks to Prof. N. V. Unnikrishnan and Dr. Santhosh Kumar of Mahatma Gandhi University, Kottayam, for the UV and photoluminescence measurements.

# References

[1] Janotti A and van de Walle C G 2009 *Rep. Prog. Phys.* **72** 126501

[2] Hwang D K, Oh M S, Lim J H and Park S J 2007 *J. Phys.* D: *Appl. Phys.* **40** R387

[3] Monakhov E V, Kuznetsov A Y and Svensson B G 2009 *J. Phys.* D: *Appl. Phys.* **42** 153001

[4] Ozgur U, Alivov Y I, Liu C, Take A, Reshchikov M A, Dogan S, Avurutin V, Cho S J and Morkov H 2005 *J. Appl. Phys.* **98** 041301

[5] Shan F K, Liu G X, Shin B C and Lee W J 2009 *J. Kor. Phys. Soc.* **54** 916

[6] Kang H S, Kang J S, Pang S S, Shim E S and Lee S Y 2003 *Mater. Sci. Eng.* B **102** 313

[7] Zhi Z Z, Liu Y C, Li B S, Zhang X T, Lu Y M, Shen D Z and Fan X W 2003 *J. Phys.* D: *Appl. Phys.* **36** 314

[8] Ohyama M, Kozuka H, Yoko T and Sakka S 1996 *J. Ceram. Soc. Jpn.* **104** 296

[9] Fujihara S, Sasaki C andKimura T 2001 *Appl. Surf. Sci.* **180** 341

[10] Znaidi L 2010 *Mat. Sci. Eng.* B **174** 18

[11] Yakuphanoglu F, Ilican S, Caglar M and Caglar Y 2007 *J. Opt. Adv. Mater.* **9** 2180

[12] Fang Z B, Yan Z J and Tan Y S2005 *Appl. Surf. Sci.* **241** 303

[13] Mahmood A, Ahmed N, Raza Q, Khan T M, Mehmood M, Hassan M M and Mahmood N 2010 *Phys. Scr.* **82** 065801

[14] Lupan O, Pauporte T, Chow L, Viana B, Pelle F, Ono L K, Roldan Cuenya B and Heinrich H 2010 *Appl. Surf. Sci.* **256** 1895

[15] Laurent K, Yu D P, Tusseau-Nenez S and Leprince Wang Y 2008 *J. Phys.* D: *Appl. Phys.* **41** 195410

[16] Prasada Rao T, Santhosh Kumar M C, Anbumozhi Angarkanni S and Ashok M 2009 *J. Alloys. Compd.* **485** 413

[17] Gupta V and Mansingh A 1996 *J. Appl. Phys.* **80** 1063

[18] Ghosh A, Deshpande N G, Gudage Y G, Joshi R, ASagade A A, Phase D M and Sharma R 2008 *J. Alloys. Compd.* **469** 56

[19] Hwang K S, Lee Y J and Hwangbo S 2007 *J. Ceramic. Proc. Res.* **8** 305

[20] Yildirim M A and Ates A 2010 *Opt. Comm.* **283** 1370

[21] Shan F K, Liu G X, Lee W J and Shin B C 2007 *J. Appl. Phys.* **101** 053106

[22] Kohen M H, Fritzche H and Ovshinky S R 1969 *Phys. Rev. Lett.* **22** 1065

[23] Damen T C, Porto S P S and Tel B 1966 *Phys. Rev.* **142** 570

[24] Wang J M and Gao L 2004 *J. Cryst. Growth* **262** 290

[25] Bagnall D M, Chen Y F, Shen M Y, Zhu Z, Goto T and Yao T 1998 *J. Cryst. Growth* **184** 605

[26] Kong D H, Choi W C, Shin Y C, Park J H and Kim T G2006 *J. Kor. Phys. Soc.* **48** 1214

[27] van Dijken A, Meulenkamp E, Vanmaekelbergh D and Meijerink A 2000 *J. Phys. Chem.* B **104** 1715

[28] Lin B, Fu Z and Jia Y 2001 *Appl. Phys. Lett.* **79** 943